

The effect of porosity size distribution on the thermal and mechanical properties of foam glasses based on silicate soda-lime waste glasses

Ehsan Shafaghat^{*1}, Ali Nemati², Azam Moosavi³, Saeed Baghshahi⁴

esila1989@gmail.com

Abstract

This study evaluated the effect of porosity size and distribution in waste soda-lime-silica glass-based foamed glasses. We chipped the glass powder grains into particles less than 70 μm . Then we prepared the ingredients with both wet and dry blending methods. To analyze the thermal behavior of glass powder and the foaming agent, we used STA. Calcium carbonate (1-7 % w/w) was added to the ingredients and exposed to 750-900 °C, followed by an examination of the foaming behavior of the samples. XRD was applied for phase assessment, and SEM was employed to evaluate the porosities' microstructure, size, and morphology. We performed the compressive strength and thermal conductivity tests on the samples. The results showed a correlation between the density of foamed glass and thermal condition process conditions as there was a reduction in the density and an increase in the porosity at 850 °C, whereas density increased and glass viscosity decreased at 900 °C. According to the results, the optimal method, ratio of foaming agent, and temperature were dry, 5 % w/w, and 850 °C, respectively. The wollastonite was crystallized after an increase in the curing temperature. In addition, due to the elevated level of density, the compressive strength reached 94.1 Mpa. The highest number of closed porosities was developed at 750 °C. In this study, low density and more closed porosities resulted in less thermal conductivity. Furthermore, the crystallization process led to reduced thermal conductivity. The minimum thermal conductivity was observed at 0.082 $\text{W}\cdot\text{m}^{-1}\cdot\text{K}^{-1}$.

Keywords: foamed glass, porosity size, low density, calcium carbonate, compressive strength, thermal conductivity

1. Introduction

Glasses are one of the highly recyclable materials in the world. Nowadays, many projects have been conducted to gather and recycle glass wastes in developed countries [1]. Foamed glasses are considered thermal insulator materials. Moreover, they benefit from biocompatibility properties and a long lifetime similar to that of construction materials, including bricks and concretes. This stability feature generates from mineral constituents and closed pores in the structure of glasses,

¹ Department of Materials Science and Engineering, Science and Research Branch, Islamic Azad University, Tehran, Iran

² Material science and Engineering Department, Sharif University of Technology, Azadi St, Tehran, Iran

³ Department of Materials Science and Engineering, Science and Research Branch, Islamic Azad University, Tehran, Iran

⁴ Department of Materials Science and Engineering, Faculty of Engineering, Imam Khomeini International University, Qazvin, Iran

bestowing them freezing tolerance and water-vapor diffusion resistance. However, foamed glasses have lower thermal insulation capacity and higher unit prices than organic foams and mineral woods; therefore, it is possible to improve their commercial applications by decreasing their development costs and enhancing their thermal insulation performance. We can produce high-quality foamed glasses by combining glass wastes and mineral substances and melting refining during manufacturing processes [2].

Foamed glasses have better physicochemical properties compared to traditional polyethylene foams, tailoring them for a wide range of thermal insulation usages. These materials have unique characteristics such as low thermal conductivity, great strength, incombustibility, high stability, and waterproofing [3]. High manufacturing costs are one of the limitations in the production of foamed glasses; using glass wastes as raw materials can be a solution to address this problem.

In a study, Petersen et al. used glass powder particles incorporated with a foaming agent to develop foamed glasses. The foaming agent induced glass porosity at high temperatures. This process generally requires a lower temperature between 650-1000 °C. In order to produce foamed glasses, it is essential to control glass composition, particles size, temperature, and type and concentration of foaming materials. There are many parameters to optimize for achieving sufficient conditions in a reasonable time. Thermal condition is the most critical parameter to control because it can significantly affect crystallization, gas formation, bubble pressure, and bubble aggregation rate [4]. In this method, we use a foaming agent inducing glass pores. The foaming process depends on the chemical decomposition of foaming agents (generally due to carbonates and sulfates release) or oxidation reactions of carbon compounds during the sintering procedure [5, 6]. The decomposition of some foaming agents results in the addition of some compounds to the glass within sintering, which may change crystallization and viscosity. Besides grain size and content, the quality and type of the foaming agent can alter the porosity and structure of foamed glasses [7]. Na₂CO₃, CaCO₃, and basic phosphate are examples of foaming agents that break down in the foamed glasses. By temperature raising and glass softening, calcium carbonate and sodium carbonate particles decompose, add calcium oxide and sodium oxide to the glass, and simultaneously release the carbon dioxide gas. The oxide settles in the melted glass bulk, acts as glass flux, and modifies its viscosity. The released CO₂ gas molecules are trapped in the glass bulk, the gas pressure increases slowly, and the melted glass bulk extends inevitably [8]. Hribar et al. exploited water glass, carbon, and Mn₃O₄ reaction to generate the foamed glass expansion. In this study, a density of 0.145 gr/cm³ was recorded [9].

Particle size is one of the efficacious parameters in foamed glass production [8]. First, the glass grains should be smaller than 0.4 mm and be sieved; otherwise, the foaming process almost holds [10]. Karamanov et al. found that a decrease of grain size significantly led to increased

density and improved condensation as two causal factors in sustaining the gas into the sample [11]. Altering the size of particles is an approach to change the porosity size distribution that may provide a heterogeneous open-porous construction by coarse particles or closed porosities using fine particles or a homogenous construction and may form open and closed porosities, according to the application [6]. König et al. mentioned the advantages of substance-substance interaction. They found that one could adequately achieve a better foaming ability mechanism of most powders using glass-foaming agent interaction, leading to a more expeditious heat-responsive reaction [12]. In another study, Ketov et al. concluded that to accomplish a satisfying condition, the size of particles should be smaller than 100 μm , and by a size reduction, the agglomeration parameter increased [13].

It is necessary to choose a proper maximum temperature for the foaming process. If we highly increase the temperature of the formed foam, the melting viscosity will become too low ($<10^3 \text{ Pa}\cdot\text{s}$). As a result, it will be too difficult to control the structure, causing the wall collapse and bubbles movement toward the surface, followed by losing the homogeneous porosity. In contrast, if the temperature is too low, glass viscosity will be too high, gas expansion becomes too laborious, and the formation of the walls will not be complete, which causes open porosities. Consequently, water absorption by the foam increases; furthermore, because the heating rate is essential for optimizing the foamed glass product, we should precisely control it. Hence, the heating rate to the foaming temperature should not be too high. The activation temperature of the foaming agent is 750-800 $^{\circ}\text{C}$. At this temperature, we observe gas production into the glass, and therefore, its volume increases [8]. Fernandes et al. indicated that density is another temperature-depended parameter; using soda-lime glass and coal ash as the foaming agents, they showed density decrease unto 850 $^{\circ}\text{C}$, and its decrease at higher temperatures, due to the decrease in viscosity [1].

Compressive strength is a primary foamed glass feature that increases with decreased porosity sizes [14]. Mugoni et al. established that we could reduce the compressive strength of foamed glass by prolonged maintenance time and higher temperature; this reduction could be due to the pre-forming and weight loss as well as pore aggregations. Porosity issues can be discussed regarding compressive strength because compression significantly depends on structure and density in the foamed glasses [15]. In addition, mechanical strength can be modified by crystals' appearance. For instance, the crystallization of glass (forming the glass product or ceramics) enhances mechanical strength. However, glass cracking may happen due to possible thermal inconsistency of crystals and matrices of the glass, resulting in compressive strength loss [16]. In the foamed glasses, having open pores reduces the mechanical strength compared to the closed ones [17].

As the primary mechanism of thermal conductivity of foamed glasses, photon transport is fragile and can be overlooked. Mean free path is a directly effective parameter for thermal

conductivity. In this case, we should decrease the mean free path of a matter to reduce its thermal conductivity, which generally causes thermal radiation of network waves and conductivity reduction. These complications include composition and structural complexity, solid solute, atomic weight differences, bond strength, grain boundary, stoichiometry, neutron radiation, impurity, and porosity. Overall, we should reconsider neutron radiation advances the crystal arrangement, which enhances the thermal conductivity. Thermal conditions can change the thermal conductivity, as temperature increase leads to thermal conductivity increase [18]. Foamed glasses can be used as thermal insulators because of their low density, low thermal conductivity, freezing tolerance, non-toxicity, non-flammability, and chemical inactivity. Teixeira et al. studied the insulation improvement techniques and found that increasing the porosity was one of the thermal conductivity factors. This parameter generally ranges from $0.08 \text{ W}\cdot\text{m}^{-1}\cdot\text{k}^{-1}$ to $0.18 \text{ W}\cdot\text{m}^{-1}\cdot\text{k}^{-1}$ [19]. The thermal conductivity of foamed glasses depends on their density in a linear mode. The thermal conductivity of silicate crystals [20] is higher than their amorphous counterparts, e.g., silicate glasses [21]. Boundary thermal resistance between crystal and glass can result in conductivity reduction of solid matter [22]. Petersen et al. found that open and closed pores are other primary factors for mechanical strength and thermal conductivity. Moreover, large porosities allow molecules to use convection in the global thermal conductivity, so thermal insulation decreases by increasing the number of open pores [16]. König et al. used black carbon and Mn_3O_4 to prepare a sample with closed pores and thermal conductivity of $0.05 \text{ W}\cdot\text{m}^{-1}\cdot\text{k}^{-1}$ [23]. Smiljanić et al. found that crystallization inhibition of the glass and using suitable additive materials could significantly decrease the thermal conductivity of the glasses [24].

This paper showed that conducting the synthesis of foamed glass with predetermined properties was possible through glass wastes. In addition, we attempted to achieve a foamed glass with homogeneous porosity; for this purpose, we distributed the foaming agent over the glass. For the last step, we studied both dry and wet blending methods, and we showed that different amounts of foaming agents and changes in the sintering temperature could alter the number and type of porosity. We investigated the effects of these conditions on the bulk density, numbers of open and closed pores, porosity size, thermal conductivity, and mechanical characteristics. The final aim of this study was to evaluate mentioned parameters for preparing foamed glass with low thermal conductivity and the proper strength. Furthermore, we used glass wastes because of their lower costs compared to conventional counterparts in the conductivity industry, with conservation of proposed properties.

2. Experimental

The glass powder is a product of soda-lime glass wastes. The report of its XRF analysis is shown in Table 1.

Table 1. Chemical analysis of the waste glass

Oxide	SiO ₂	Na ₂ O	CaO	MgO	Fe ₂ O ₃	Al ₂ O ₃	K ₂ O
%wt	72.50	11.20	8.46	5.60	1.10	1.0	0.24

Table 2. The samples prepared in this work

Synthesis method	Temperature	Foaming agent			
		1%	3%	5%	7%
Dry method	C°750	1%D750	3%D750	5%D750	7%D750
	C°800	1%D800	3%D800	5%D800	7%D800
	C°850	1%D850	3%D850	5%D850	7%D850
	C°900	1%D900	3%D900	5%D900	7%D900
Wet Method	C°750	1%W750	3%W750	5%W750	7%W750
	C°800	1%W800	3%W800	5%W800	7%W800
	C°850	1%W850	3%W850	5%W850	7%W850
	C°900	1%W900	3%W900	5%W900	7%W900

In the dry method, for 5 hours, we chipped the powder grains into particles less than 70 μm by the speed milland different mass fractions of calcium carbonate (1%, 3%, 5%, and 7% w/w) were added to the powder. In the wet method, for 1 hour, we add glass powder to the foaming agent (1%, 3%, 5%, 7% w/w) and water (50% w/w). Then, to dry the samples, we placed them into the dryer for 5 hours and 90 °C. To apply raw strength, compressibility, and better quality of raw materials, we granulated the prepared samples with polyvinyl alcohol 0.5%. The obtained glass powders (15 gr) were inserted in a cylindrical mold and pressed under 35 MPa by a manual uniaxial hydraulic press. The prepared samples were tablets with a diameter of 30 mm and a height of 10mm.

To evaluate the behavior of prepared tablets, we placed them into an electric furnace at 750 °C, 800 °C, 850 °C, and 900 °C with a heating rate of 5 °C/min and maintenance at the maximum temperature for 30 minutes. Then, tablets were naturally cooled to room temperature in the furnace. To evaluate the thermal behavior of raw materials, we used simultaneous thermal decomposition analysis (STA STA-PL1640; United Kingdom). This analysis used alumina powder as the reference sample, ait atmosphere, and the heat rate of 10 °C/min. To evaluate the physical properties of

foamed samples, we measured and discussed the diagonal and thickness expansions, foaming factor, theoretical density, bulk density, rational density, percentage of general, closed, and open porosities. The compressive strength of prepared foamed glasses was measured using SANTAM (STM20) at a 1 min/mm loading rate. The compressive strength of the foamed glass samples was calculated from seven cut and flattened samples. This value was obtained from Equation 1.

$$S = \frac{W}{A} \quad (1)$$

Where S was compressive strength (MPa), W denoted weight force (N), and A was cross-section (mm^2).

To evaluate and identify the forming of the crystal phases after thermal processes, we used X-ray monochrome radiation (Siemens D-5000) of Cu-K α with a wavelength of 1.5405 Å. We performed from a starting point of 5.01 degrees to the endpoint of 79.990 degrees with a step size of 0.02 and a pause time of 0.5 s for each step. Crystal phases were determined by XPert-HighScore-Plus-3.0. All 32 prepared samples foamed in different conditions were evaluated with optical microscopy (OM). Then we used FESEM scanning electron microscopy (MRIA3 TESCAN; Czech Republic) to evaluate better the microstructure and shape of porosities in the optimum samples. Before the test, the surface of the samples was smooth and polished and filmed by the gold. We used image J software to estimate the pore size by measuring the 50 pores of each sample and averaging them. We employed the mixture of chipped glass powder and calcium carbonate (5%) as the foaming agent to assess the grain size by FESEM scanning electron microscopy. Also, we conducted energy-dispersive X-ray spectroscopy (EDS) for elemental analysis of two points of the raw material powders. To appraise the thermal conductivity, we used a xenon light flash thermal conductivity apparatus (XFA 500; Linseis; Germany). XFA includes furnace, temperature controller, xenon lamp, thermocouple, IR detector, and sample holder. The samples were prepared in a square shape with a side of 10 mm and a thickness of 1 mm. In XFA, samples are exposed to the high intensity of energy pulses in a short period; the samples' surfaces absorb the energy of these pulses; finally, thermal diffusion is calculated by the samples' thickness and time required to increase the temperature of another surface of the sample. Regarding thermal diffusion (α), specific heat capacity (C_p), and sample density (ρ) in the specific test temperature, we can calculate the thermal conductivity of the sample using Equation 2.

$$K(T) = \alpha (T) \cdot C_p(T) \cdot \rho (T) \quad (2)$$

3. Results and discussion

Thermal analysis is an efficient method to predict the thermal characteristics of foaming agents. We used STA to evaluate the thermal behavior and crystallization of glass powder and obtain the required data of the foaming agent to continue the procedure. We conducted the thermal analysis to achieve the behavior pattern of the foaming agent (calcium carbonate) and the glass powder as well schemed in Figures 1a and b, respectively.

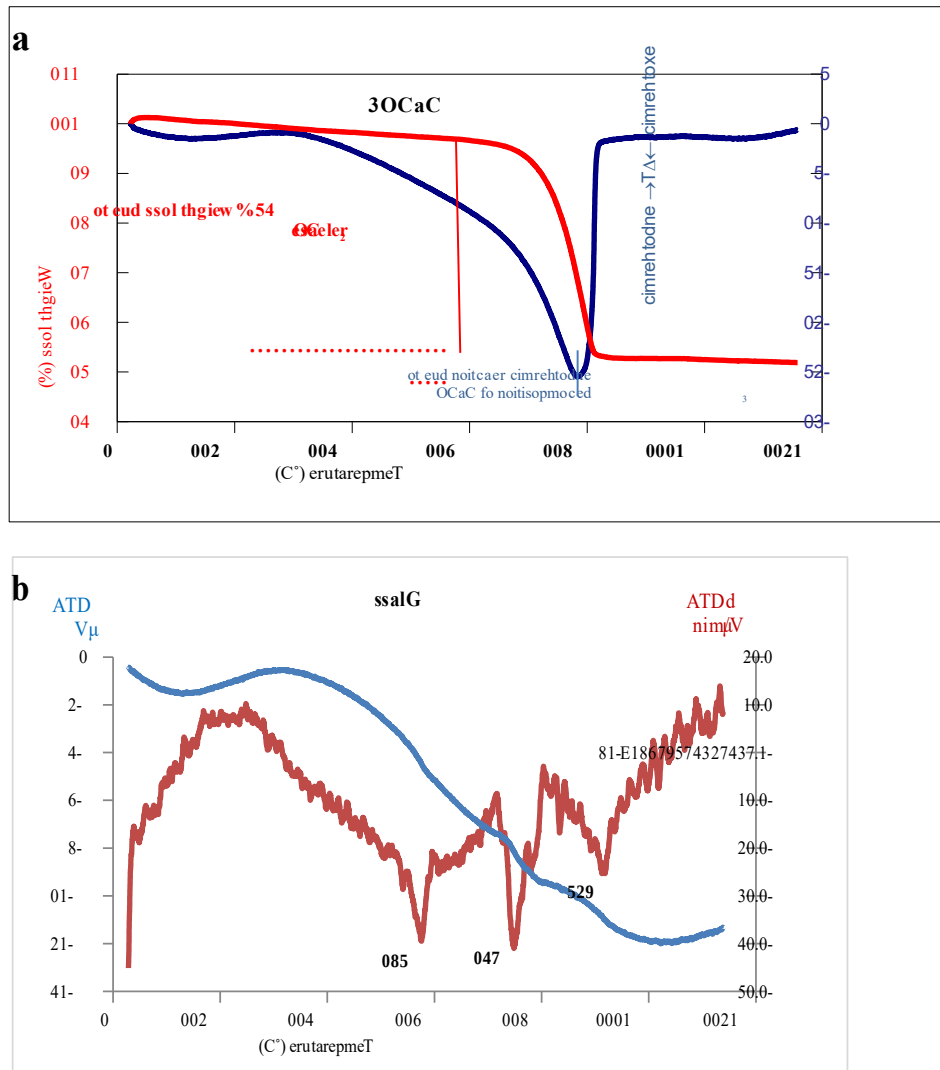


Figure 1. STA of (a) calcium carbonate, and (b) primary glass powder

As shown in Figure 1a, in the TGA graph, the temperature of weight loss ranges from 650 °C to 850 °C, and its measure is 45% and is a result of CaCO_3 decomposition and the release of CO_2 . There is a sharp endothermic peak at 780 °C in the DTA graph of calcium carbonate, which is in the TGA's weight loss range and formed by the decomposition of CaCO_3 . Figure 1b shows several slope changes which were plotted to have a better dDTA analysis. Sintering temperatures of foamed glass were designed from 750 °C to 900 °C, according to the peaks at 580 °C, the temperature of

transition to the glass form (T_g), 740 °C, the temperature of glass crystallization (T_c), and 925 °C, the melting point of the glass (T_s).

The strong effect of particle size on the foamed glass synthesis causes gas discharging and no gas retention due to the distance between the glass grains. As shown in Figure 2, the glass grains were chipped below 70 μm and formed the average highest particle size of 23 μm . This particle size can synthesize enhanced foamed glass because better compression leads to increased density before sample sintering and better retention of foaming agent in the glass, which is essential to synthesize a foamed glass with a very low density.

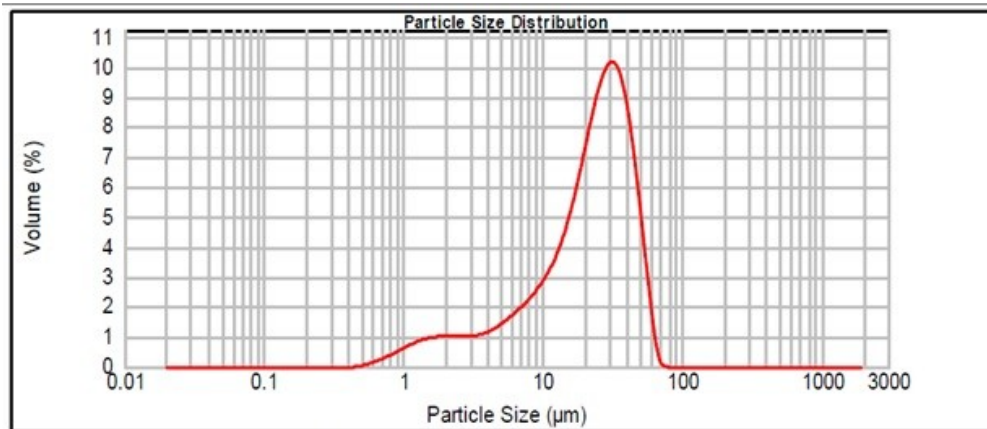


Figure 2: Particles size distribution of glass powder

To investigate the samples' physical properties and foaming behavior from 750 °C to 900 °C with dry and wet mixing methods, we measured the linear expansion in diameter and thickness, bulk density, foaming factor, and closed pore percentage. In both dry and wet methods, diameter expansion increased due to the increased gas pressure after increasing the porosities' temperature. In all fractions, the slope of expansion was almost the same except for the 7% w/w, which was less than other fractions, which could be due to more amount of foaming agent and more possibility of shorter distances of foaming agent in the field and more porosity bonding, which the latter could weaken the porosity walls, crack the wall and release the gas which is a factor to less expansion than other fractions of foaming agent. The rate of expansion in the dry method is more than that of the wet method. Moreover, most of the thicknesses in both methods has increased, but we should take into account the higher percentage of the thickness expansion in Figure 4 compared to the percentage of diameter expansion in Figure 3, whose reason is the tendency of leaving gases to move toward the surface due to the downward pressure of molten masses. At 900 °C, along with a decrease in the glass viscosity, some of the increased thickness begins to decrease, reducing the thickness at this temperature compared to 850 °C, which has the highest thickness in different fractions of foaming agent.

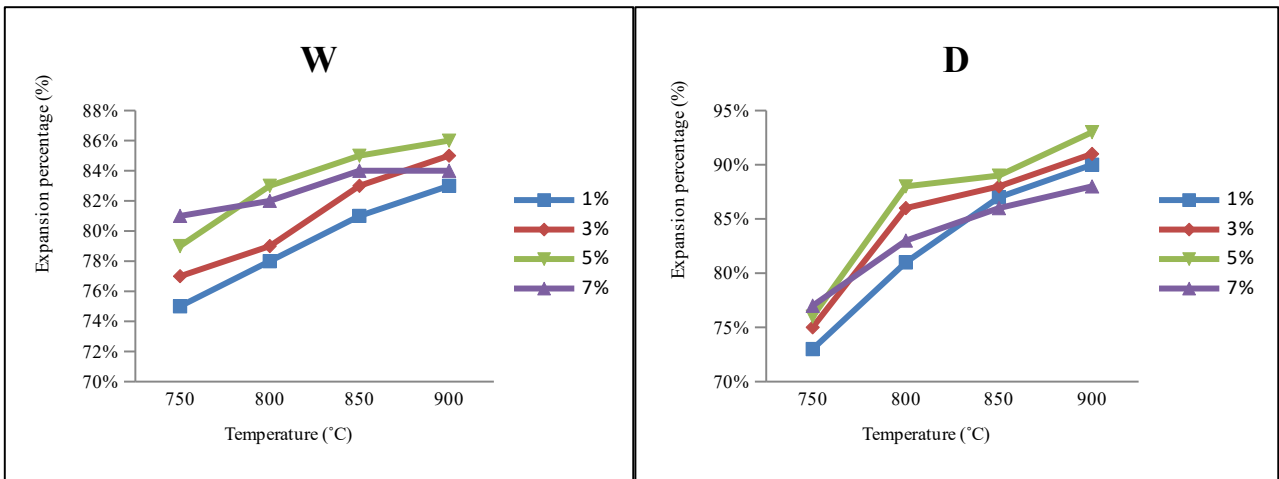


Figure 3. Percentage of diameter expansion of samples at sintering temperature in dry mixing (D) and wet mixing (W)

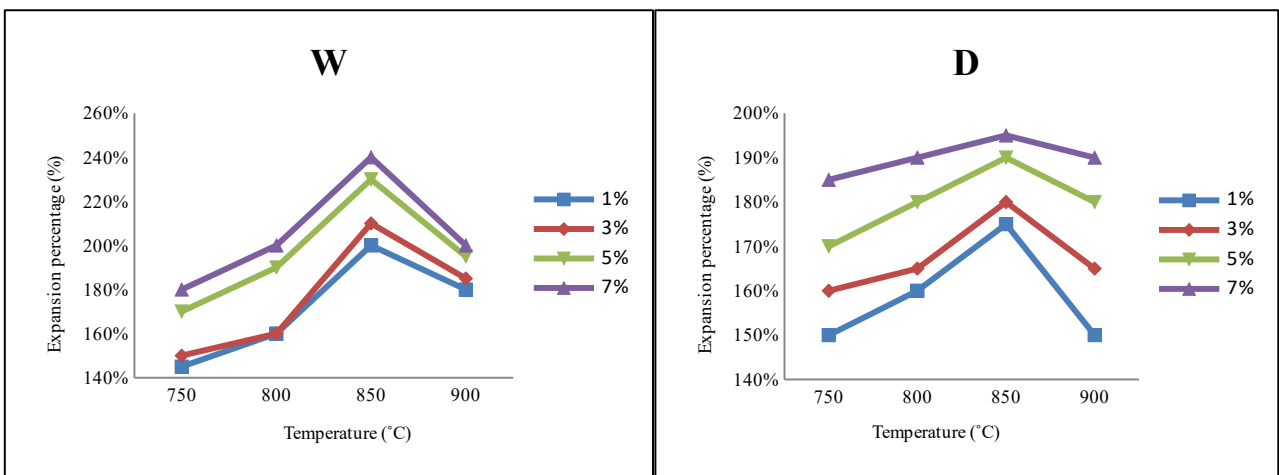
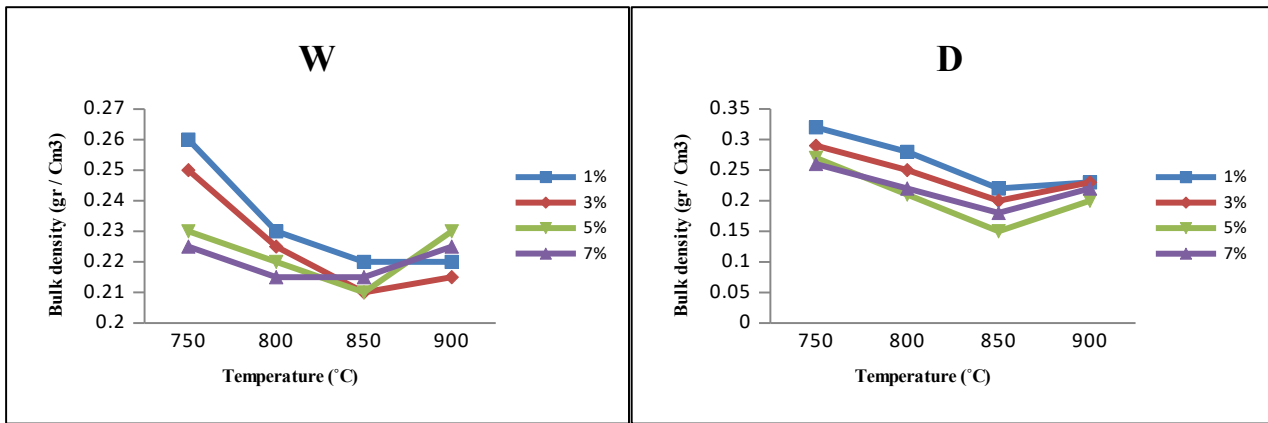


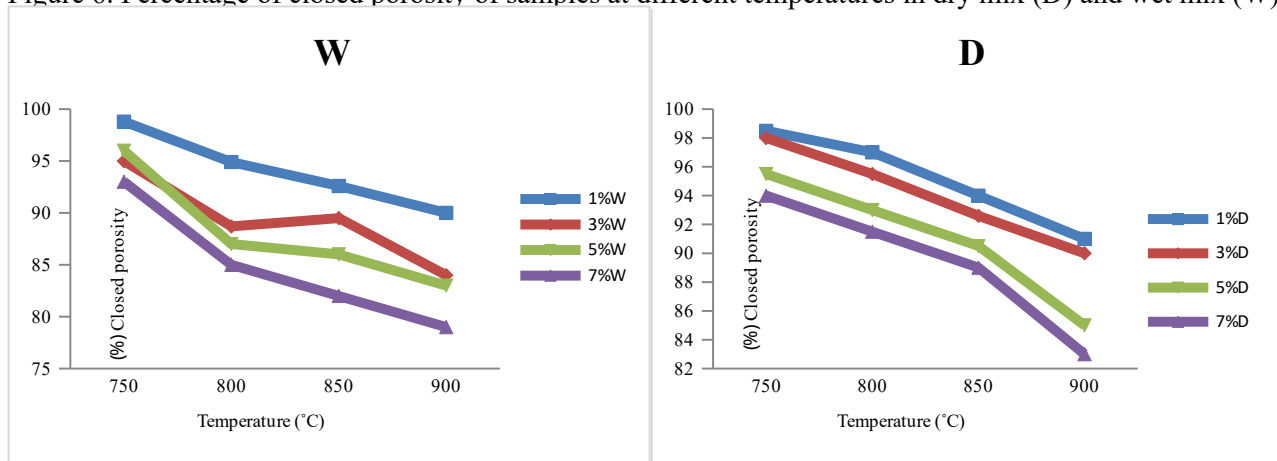
Figure 4. Percentage of thickness expansion of samples at sintering temperature in dry mixing (D) and wet mixing (W)

we can conclude that as the temperature increases, the volume increases due to more decomposition of foaming agent and gas formation and the porosity in the glass, and finally, the sample bulk density decreases. Only at 900 °C, as there was a sample thickness contraction at this temperature, there was a slight increase in bulk density due to a reduced viscosity and porosity degradation resulting in a density increase. The presence of more wollastonite phase causes greater wall strength which prevents the increase in the porosity volume that is the reason for higher densities in the higher percentages. In the dry method, the density is lower than the dry method due to the agglomeration of calcium carbonate particles, which joins pores together and combines them and releases the gas, and does not allow the density to decrease as much as the dry method.



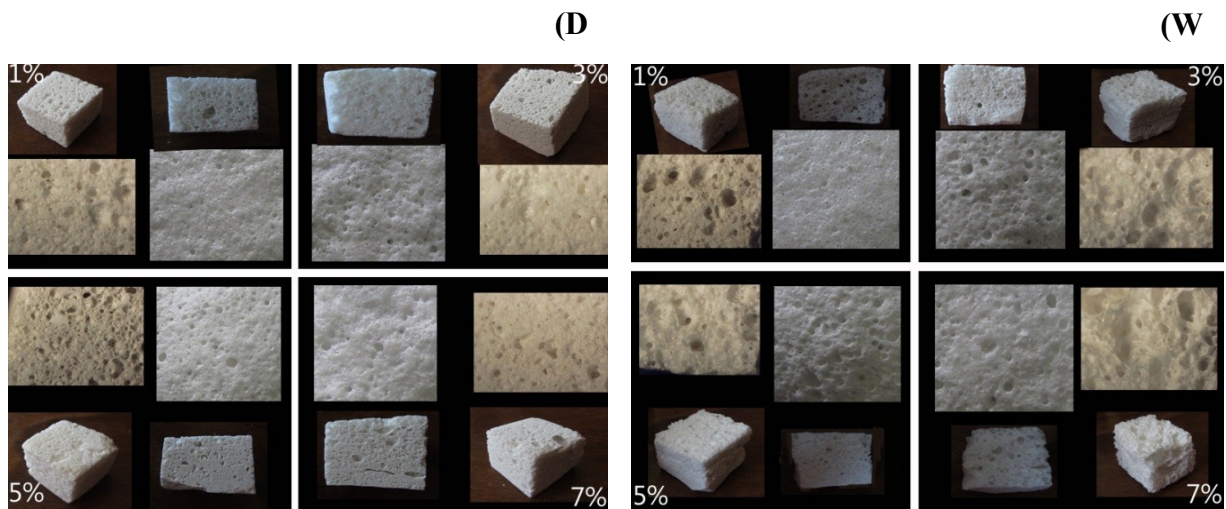
Similarly to our study, Abdollahi et al. concluded that an increase in temperature is directly related to a decrease in density that happens as a result of greater oxidation of foaming agent in the presence of oxidizing agents in the higher temperatures and the increase in gas pressure in the sample [25]. Owoeye et al. found that an increase in the temperature from 800 °C to 850 °C reduces the density by about 7.17% for powder grains with a size of 150 μm which indicates a decrease in sample density at the effect of higher porosities; we found similar results in our study [26].

Figure 6. Percentage of closed porosity of samples at different temperatures in dry mix (D) and wet mix (W)



One of the most critical factors for the properties of foamed glasses is the presence of closed porosities that reveals the quality of an insulator. The percentage of samples' closed pores is plotted in Figure 6 regarding the temperature of heat treatments. The general scheme in all fractions of foaming agents is decreasing by the increase in the temperature. The increase in sintering temperature causes the increase in gas pressure in the pores, walls deconstruct, and the number of closed pores decreases. The difference between the amounts of foaming agents in closed pores in the dry and wet methods is due to inconsistency in the agglomeration graph of different foaming agents. Still in the dry method, as the number of foaming agents increases, the number of closed pores decreases. Higher amounts of foaming agents increase the likelihood of joining the pores, which also cause contact with the outside and create open pores.

Most studies reported foamed glass with partially closed pores and partially with open pores or transition from masses with higher density to masses with lower density and open pores. [16, 27, 28] König et al. found that the density of samples with closed pores can be controlled by changing the temperature [29]. We can indicate that thermal conductivity by materials with open pores is higher than materials with closed pores [30]. Pores should be closed to be utilized in thermal insulation applications, while open pores can be used in acoustic insulation applications. Usually, the open pore limiting values for closed and open pores of the foams is a maximum of 20% and a minimum of 90%, respectively. König et al. used panel glass to prepare samples with a density of 120 kg.m^{-3} , including 98% of closed pores and 110 kg.m^{-3} reaching 8% of open pores, which are similar to our results [31]. Petersen et al. used a carbon foaming agent, which in all percentages of carbon by an increase in temperature the number of closed pores decreased [32].



In Figure 7, the images of samples at $750 \text{ }^\circ\text{C}$ in dry and wet methods show regular, smaller, and more closed pores in the wet method, which is more desirable for synthesizing foamed glass. According to the results in the images shown in the dry method, density and number of porosity and percentage of closed pores have adverse effects on the final foamed glass due to the agglomeration of the foaming agent particles and creation of irregular and coarse pores. Then, we use the dry method as the optimal method to use foaming agent 5% w/w at $850 \text{ }^\circ\text{C}$. We use this condition because of the lowest density and the highest number of porosities as the optimizing factors.

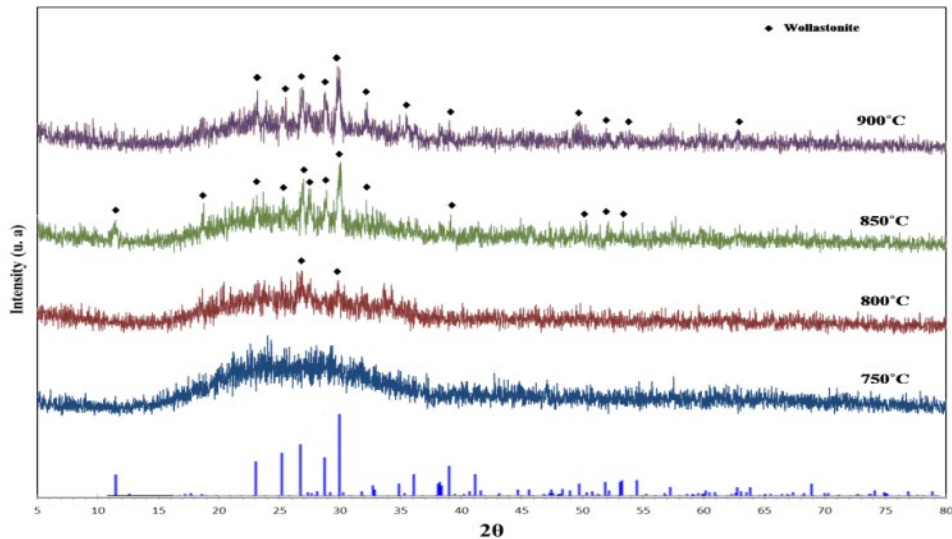
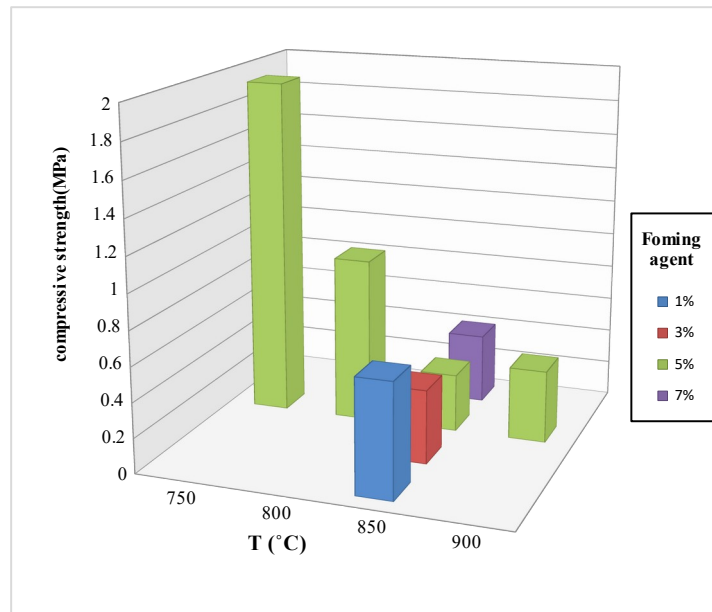


Figure (8): X-ray diffraction pattern of glass foam with 5% by weight of

To evaluate the crystalline phases in the sintered samples at 750-900 °C with 5% by weight of foaming agent, we conducted the XRD test as shown in Figure 8. The formation of crystalline phases and their relationship to the used composition and the sintering temperature are two factors that determine the final properties of foamed glasses. In Figure 8, XRD patterns show that the general scheme of peaks is amorphous, and crystalline phase wollastonite appeared with standard card (ICDD 1460-043-00) at 850 °C and 900 °C and in a lesser amount at 800 °C. According to CaCO_3 as the foaming agent which decomposes by a heat treatment for foamed glass synthesis and causes the creation of wollastonite (CaSiO_3) phase. Fernandes found XRD patterns collected for each sample show foamed glasses are initially amorphous and are showing only a broad and weak XRD peak of quartz phase at 650 °C and 750 °C which we can observe quartz phase at 750 °C indicating quartz phase is not visible above this temperature and with increasing temperature the wollastonite phase is seen the result of which is similar to the present study [33]. Monich et al. also noticed the wollastonite phase in their synthesized foamed glass and indicated that wollastonite is a phase that is observed in soda-lime silicate glasses [34].



Compressive strength of foamed samples in different temperatures with a fixed mass fraction of 5% foaming agent and samples with different mass fractions at a constant temperature of 850 °C measured as shown in Figure 9. Compressive strength is directly related to foam density, and owing to increases in the density, it increases and is reversely related to the foaming factor and porosity of the sample and the more porosity thinning and weakening of the foam cell walls thus the compressive strength will decrease. As shown in Figure 9, temperature increase was one of the factors which decreased the density in the samples 750 °C to 900 °C in the fixed foaming agent (5% w/w), through which increasing temperature due to higher porosity, compressive strength decreases. However, at 900 °C, the strength increases with increasing the density, due to the reduction of viscosity, porosity loss and consequently increase. It has been density that will increase compressive strength. According to Figure 9, by 1-5%, foaming agent strength decreased by creating more porosity, but in the higher percentages (>7%) of foaming agent, porosity does not increase by wollastonite phase forming, and intrinsic strength of wollastonite increases strength at this temperature. Compressive strength obtained in this study is comparable to commercial counterparts and has the same strength required for construction purposes. Increasing the amount of foaming agent reduces compressive strength due to an increase in porosity.

The higher the porosity and the lower the density, the lower the strength because applied loading in the sample is distributed among smaller glass surfaces and reduces the compressive strength [7]. Similar to our results König et al. stated that critical parameters for maintaining preferred mechanical properties resulting in load-bearing capability include high density, small pore sizes, and homogeneous size distribution [31].

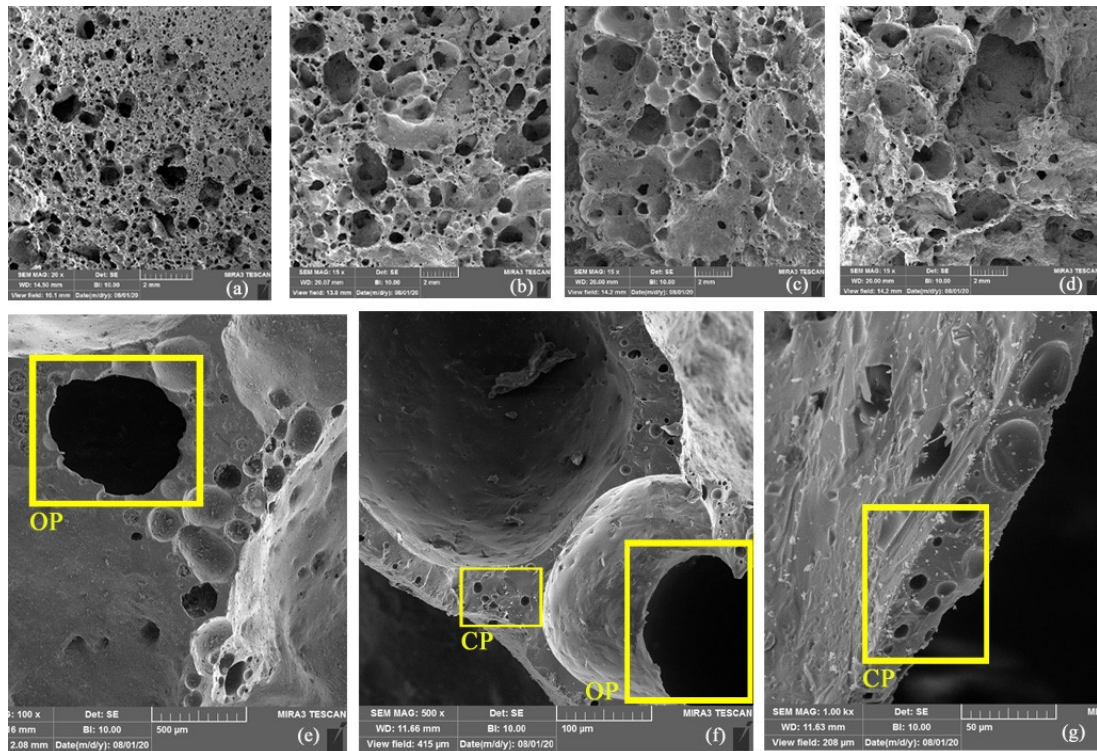


Figure 10. FESEM image of produced foam glass: (a) 5% 750°C (b) 5% 800°C (c) 5% 850°C (d) 5% 900°C (e) 1% 850°C (f) 3% 850°C (g) 7% 850°C

We provided FESEM images to evaluate the size, shape, and distribution of porosities in the dimension of cut sections of foamed glass samples. There are more fine closed pores in sample 5D750 in Figure 10a due to the lower temperature of the heat treatment while being large by increasing temperature in Figure 10b, c, and d. We can observe the merging of fine porosities, which then become more coarse. The pressure within fine pores is higher than coarse pores resulting flow of fine pores toward coarse pores in a way that they disappear, and this conversion reduces the surface energy of the system. Figure 10d shows the open pores with sharp edges of the walls and inertly connected to other pores of foamed glass with high sintering temperature and crystalline phase forming as the formulation factors obtained by XRD results. At 900 °C, the flow of glass increases is accompanied by the fall of porosities and deformation of most spherical porosities. Closed pores are generally spherical which their shape is removed by the pressure of the surrounding pores and then become open pores.

FESEM image (Figure 10e and f) of the sample 1D850 shows many closed and a few open pores attributed as OP. There are sharp edges of a pore that indicates the rupture of the pore cell wall due to the high pressure of the gas, which forms open pores. The high pressure of the gas inside the porosities can also be observed in the closed pores of these shapes, which reshaped them. However, in some pores, due to the thinness of the cell and gas pressure inside the cell, it causes the perforation of spherical cells. In this study, by the highest fraction of foaming agent, in sample 7D850, which is shown in Figure 10g-CP, we can see close pores in the walls, but coarse open pores

are also observed. The higher fractions of the foaming agent in this sample can increase crystallization in the system. The presence of the crystalline phase is one of the factors causing open porosity; when the crystalline phase is formed in the cell walls, by an increased temperature and pressure of the gas inside the cell, the porosity size increases, which itself increases the pressure of the porosity gas, resulting in the destruction of the cell wall and forming of open porosity. Zhang et al. found that increasing the number of foaming agents increases interconnected pores and gas pressure, leading to larger porosities. The larger size of porosities was the main reason for the change in density and strength [35]. These results are similar to the finding of our study. Chen et al., in their research, reported that specifically, pores found in some samples were coarse and not spherical shaped, significantly reducing mechanical strength. Pores in another sample were more homogeneous, regular, and fine, improving the insulation properties of foamed ceramics. Increased viscosity also increases the resistance against pore growths [36]. König et al. reported that an increase in pore size could be observed along with reduced density. The analysis results of pore sizes and distribution were extracted from SEM images; the researchers found that the reduction of density increases the size of the pores, and the distribution extends, which is similar to the results of the present paper [31].

We used Image Processing and Analysis in Java (Image J) to evaluate porosity size in samples' FESEM images, as is shown in Figure 11. Size of new porosities is directly related to the heat treatment temperature, and as is shown in Figure 11, by increasing the temperature of the procedure, the porosity size has increased. The least average porosity size in samples with 5% w/w of the foaming agent at 750 °C was 46 µm, and the largest average size at the same fraction of the foaming agent has belonged to the highest sintering temperature at 900 °C that was 1.042 mm.

König et al. estimated the pore sizes by Image J with an average of 0.50 mm to 1.31 mm. The increase of pore size depends on higher pore pressure and lower glass viscosity at the higher temperature, affecting the expansion of initially formed pores and the fusion of pores. In particular, the coalescence is promoted with an increase in the foaming temperature and the foaming time. Regarding the relationship between density and grain size, the average size of porosity increases by density reduction in the foamed glasses, whose results are similar to our study [31]. Cimavilla-Román et al., similar to the present study, concluded that as porosity increases, the average pore cell size and open-pore content increase, which is most likely the result of cellular degradation mechanisms that lead to cellular degradation cell fusion and ruptures of cell walls [37].

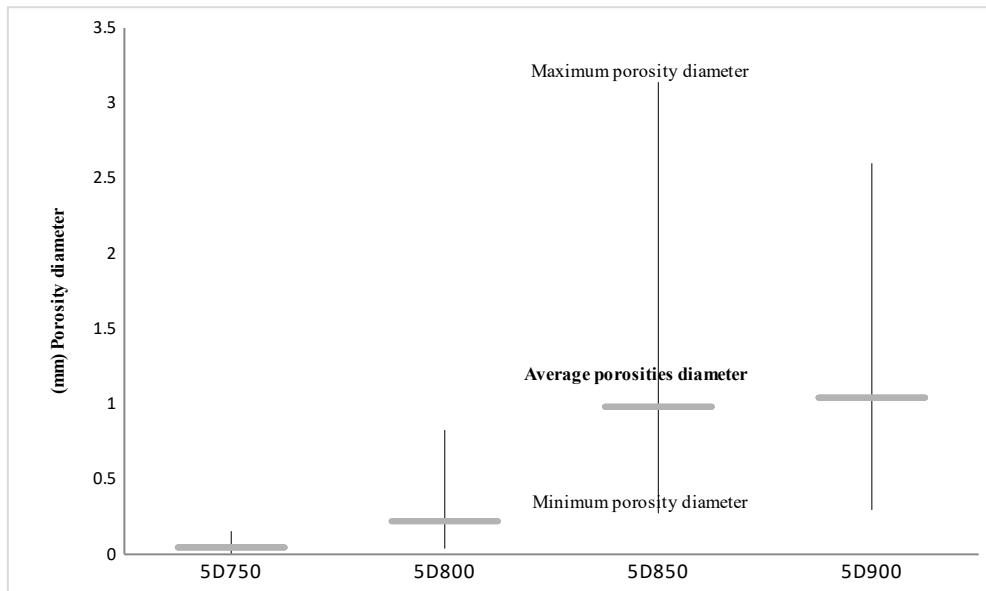
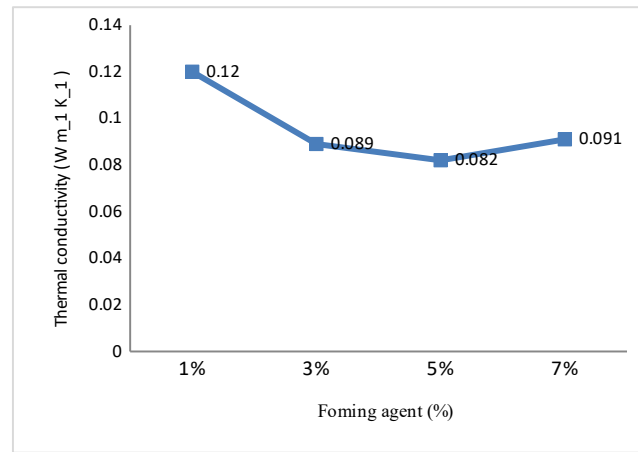
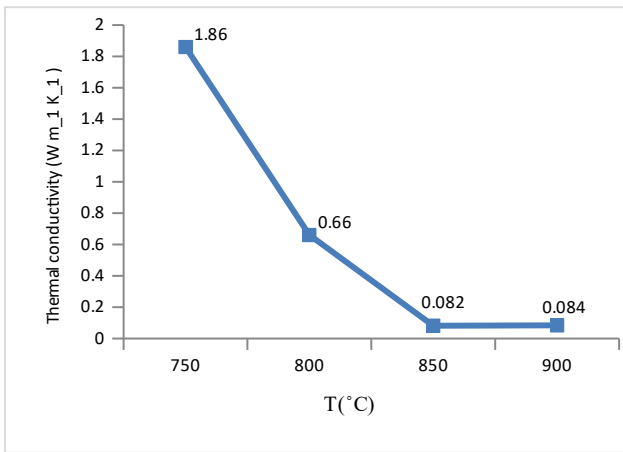


Figure 11. average porosity size of 5% weight samples of foaming agent at different temperatures of heat treatment graph

XFA measured the thermal conductivity of foamed glasses, and as is shown in Figure 12, the process of decreasing thermal conductivity has been raised by an increase in temperature and the number of pores. At 900 °C, pore loss results from glass viscosity increase, and this loss causes thermal conductivity improvement than the sample with a sintering temperature of 850 °C. Figure 13 shows that thermal conductivity has decreased in the range of 1-5 % because porosities increased. Nevertheless, in 7%, the appearance of the crystalline phase, which reduces total porosity and increases the number of open pores, increases the thermal conductivity. Additionally, the intrinsic thermal conductivity of crystals is higher than the glass due to irregularity in the glass. Thermal conductivity decreases linearly by reducing the density of all samples, in which closed porous samples have lower thermal conductivity than the open porous sample with the same density. The lowest thermal conductivity of closed porous samples has been measured in samples with the lowest density. Thermal conductivity is transmitted in the solid and gas phases [38]. Østergaard et al. found that thermal conductivity was transmitted mainly in the solid phase, and the overall thermal conductivity in the solid foamed glass is caused by solid glass, crystallin content, and open porosities. The thermal conductivity of porous and molten samples indicates the highest and lowest thermal conductivity of the solid phase of foamed glasses prepared by these foaming agents. The content of glass-soluble foaming agents has a significant impact on thermal conductivity. Generally, with the addition of foaming agent, thermal conductivity improved enhances, similar to Figure 13. Samples containing crystalline phases have higher thermal conductivity than pure glass phases [39].



4. Conclusion

The exploitation of silica-soda-lime glass wastes showed great results close to commercial foamed glass standards. This fact has promising advantages in saving natural resources and recycling wastes. Employ of CaCO₃ foaming agent alone by decomposition, inserted CO₂ gas into the glass which caused porosity and synthesis of foamed glass that the mass fraction of 5% w/w of foaming agent showed relatively more favorable results at all sintering temperatures compared to other fractions. Due to the agglomeration of CaCO₃ particles, the wet mixing method did not form regular porosities, while the dry method produced regular porosities. The increase in the sintering temperatures of 750-900 °C that was performed for all foaming percentages could enhance the decomposition of the foaming agent. As a result, more pores were produced, but at 900 °C, the number of pores decreased because viscosity decreased and pore walls fell, and finally, density has increased. The grain size of glass strongly affects the formation and foaming of the sample. After chipping grains below 70 μm, density increased due to better compression at the time of gas formation, the foaming agent was retained in the glass in a better way, and this factor was favorable to the synthesis of the low-density foamed glasses. The highest number of closed pores was at 750 °C, where gases had the highest degree of retention in the field of the glass, and as the temperature increased, the number of open pores increased, and the closed pores were reduced. In XRD assessment, it was observed that the increasing temperature wollastonite phase crystallized because CaO was inserted into the glass by calcium carbonate decomposition. Compressive strength is directly related to the foam density and is inversely related to the number of pores in the sample, and the higher number of pores of the sample, the thinner and weaker the cell walls of the foamed glass; thus, the compressive strength will be decreased. As the heat treatment temperature increases, the size of pores increases. The smallest average size of the pores by 5% w/w of the foaming agent was 46 μm at 750 °C, and the largest average size by the same foaming agent mass fraction was

1.042 mm at 900 °C. In FESEM images, it was found that fine pores surrounded the coarse pores by placement in the cell walls. The size of pores is directly related to heat treatment temperature with a fixed number of foaming agents. In this case, samples with closed pores have less thermal conductivity with the same density. The content of glass-soluble foaming agents is another crucial factor affecting the thermal conductivity of the solid phase of the glass. In general, the thermal conductivity increases with the addition of a foaming agent. Samples containing crystalline phases have higher thermal conductivity than pure glass phases. This study found the best thermal conductivity in an insulating sample of $0.082 \text{ W}\cdot\text{m}^{-1}\cdot\text{K}^{-1}$ which is desirable according to commercial foamed glass standards. The heat is transmitted through the solid phase of the glass and the gas phase of the porosity, which in this case, the solid factor is more effective than the gas phase. Aside from utilizing the waste glass, which leads to a reduction in the production costs, The foamed glass designed in this research was able to meet the international standards and contain the required properties. This product can be used as an excellent renewable insulator in the insulation industry for construction.

References

1. Fernandes, H., D. Tulyaganov, and J. Ferreira, Preparation and characterization of foams from sheet glass and fly ash using carbonates as foaming agents. *Ceramics International*, 2009. 35(1): p. 229-235.
2. König, J., et al., Suppressing the effect of cullet composition on the formation and properties of foamed glass. *Ceramics International*, 2018. 44(10): p. 11143-11150.
3. Liu, T., et al., Phase evolution, pore morphology and microstructure of glass ceramic foams derived from tailings wastes. *Ceramics International*, 2018. 44(12): p. 14393-14400.
4. Petersen, R.R., J. König, and Y. Yue, The viscosity window of the silicate glass foam production. *Journal of Non-Crystalline Solids*, 2017. 456: p. 49-54.
5. Studart, A.R., et al., Processing routes to macroporous ceramics: a review. *Journal of the American Ceramic Society*, 2006. 89(6): p. 1771-1789.
6. Souza, M.T., et al., Glass foams produced from glass bottles and eggshell wastes. *Process Safety and Environmental Protection*, 2017. 111: p. 60-64.
7. Spiridonov, Y.A. and L. Orlova, Problems of foam glass production. *Glass and ceramics*, 2003. 60(9-10): p. 313-314.
8. Scheffler, M. and P. Colombo, *Cellular ceramics: structure, manufacturing, properties and applications*. 2006: John Wiley & Sons.
9. Hribar, U., M. Spreitzer, and J. König, Applicability of water glass for the transfer of the glass-foaming process from controlled to air atmosphere. *Journal of Cleaner Production*, 2021. 282: p. 125428.
10. Ducman, V. and M. Kovacevic, *The foaming of waste glass*. 1997.
11. Karamanov, A., et al., Sintered glass-ceramics and foams by metallurgical slag with addition of CaF_2 . *Ceramics International*, 2020. 46(5): p. 6507-6516.

12. König, J., R.R. Petersen, and Y. Yue, Fabrication of highly insulating foam glass made from CRT panel glass. *Ceramics international*, 2015. 41(8): p. 9793-9800.
13. Ketov, A., An experience of reuse of a glass cullet for production of foam structure material, in *Recycling and Reuse of Glass Cullet*. 2001, Thomas Telford Publishing. p. 85-91.
14. Morgan, J., J. Wood, and R. Bradt, Cell size effects on the strength of foamed glass. *Materials science and engineering*, 1981. 47(1): p. 37-42.
15. Mugoni, C., et al., Design of glass foams with low environmental impact. *Ceramics International*, 2015. 41(3): p. 3400-3408.
16. Petersen, R.R., J. König, and Y. Yue, The mechanism of foaming and thermal conductivity of glasses foamed with MnO₂. *Journal of Non-Crystalline Solids*, 2015. 425: p. 74-82.
17. Gibson, L.J. and M.F. Ashby, *Cellular solids: structure and properties*. 1999: Cambridge university press.
18. Kingery, W.D., *Introduction to ceramics*. 1976.
19. Teixeira, L., et al., Vitrocrystalline foams produced from glass and oyster shell wastes. *Ceramics International*, 2017. 43(9): p. 6730-6737.
20. Horai, K.i., Thermal conductivity of rock-forming minerals. *Journal of geophysical research*, 1971. 76(5): p. 1278-1308.
21. Varshneya, A.K., *Fundamentals of inorganic glasses*. 2013: Elsevier.
22. Smith, D.S., et al., Thermal conductivity of porous materials. *Journal of Materials Research*, 2013. 28(17): p. 2260-2272.
23. König, J., et al., Application of foaming agent–oxidizing agent couples to foamed-glass formation. *Journal of Non-Crystalline Solids*, 2021. 553: p. 120469.
24. Smiljanić, S., et al., Influence of additives on the crystallization and thermal conductivity of container glass cullet for foamed glass preparation. *Ceramics International*, 2021.
25. Abdollahi, S. and B.E. Yekta, Prediction of foaming temperature of glass in the presence of various oxidizers via thermodynamics route. *Ceramics International*, 2020.
26. Owoeye, S.S., et al., Preparation and characterization of foam glass from waste container glasses and water glass for application in thermal insulations. *Ceramics International*, 2020.
27. García-Ten, J., et al., Glass foams from oxidation/reduction reactions using SiC, Si₃N₄ and AlN powders. *Glass Technology-European Journal of Glass Science and Technology Part A*, 2011. 52(4): p. 103-110.
28. Llaudis, A.S., et al., Foaming of flat glass cullet using Si₃N₄ and MnO₂ powders. *Ceramics international*, 2009. 35(5): p. 1953-1959.
29. König, J., et al., Evaluation of the contributions to the effective thermal conductivity of an open-porous-type foamed glass. *Construction and Building Materials*, 2019. 214: p. 337-343.
30. Schuetz, M. and L.R. Glicksman, A basic study of heat transfer through foam insulation. *Journal of Cellular Plastics*, 1984. 20(2): p. 114-121.
31. König, J., et al., Synthesis and properties of open-and closed-porous foamed glass with a low density. *Construction and Building Materials*, 2020. 247: p. 118574.
32. Petersen, R.R., et al., The foaming mechanism of glass foams prepared from the mixture of Mn₃O₄, carbon and CRT panel glass. *Ceramics International*, 2021. 47(2): p. 2839-2847.
33. Fernandes, H.R., et al., Environmental friendly management of CRT glass by foaming with waste egg shells, calcite or dolomite. *Ceramics International*, 2014. 40(8): p. 13371-13379.

34. Monich, P.R., et al., Porous glass-ceramics from alkali activation and sinter-crystallization of mixtures of waste glass and residues from plasma processing of municipal solid waste. *Journal of Cleaner Production*, 2018. 188: p. 871-878.
35. Zhang, C., et al., Preparation and properties of foam ceramic from nickel slag and waste glass powder. *Ceramics International*, 2020. 46(15): p. 23623-23628.
36. Chen, Z., et al., Reuse of mineral wool waste and recycled glass in ceramic foams. *Ceramics International*, 2019. 45(12): p. 15057-15064.
37. Cimavilla-Román, P., et al., Modelling of the mechanisms of heat transfer in recycled glass foams. *Construction and Building Materials*, 2021. 274: p. 122000.
38. Skochdopole, R., The thermal conductivity of foamed plastics. *Chemical Engineering Progress*, 1961. 57(10): p. 55-59.
39. Østergaard, M.B., et al., Influence of foaming agents on solid thermal conductivity of foam glasses prepared from CRT panel glass. *Journal of Non-Crystalline Solids*, 2017. 465: p. 59-64.